

Ethylene Adsorption and Coadsorption with H on Pd(110) from First Principles

J.-S. Filhol, D. Simon,* and P. Sautet

Laboratoire de chimie théorique et des matériaux hybrides, École Normale Supérieure de Lyon,
46 allée d'Italie, 69364 Lyon Cedex 07, France and Institut de Recherches sur la Catalyse, CNRS,
2 avenue A. Einstein, 69626 Villeurbanne Cedex, France

Received: July 31, 2002; In Final Form: November 12, 2002

The adsorption of ethylene on a Pd(110) surface and the coadsorption with hydrogen is investigated using gradient corrected periodic density functional calculations. The surfaces have been modeled by 6 layers of Pd atoms for different unit cell sizes and geometries allowing us to study ethylene coverages from 0.125 to 0.5 monolayer (ML) and hydrogen from 0.125 to 1.0 ML. The adsorption energy and the geometry have been computed for different adsorption sites (on top of a Pd or bridging two Pd atoms) for different coverages. For bare Pd surfaces, at any coverage, the bridge site is always found to be more stable than any other site. This result is in contradiction with former interpretations of vibrational spectra. The validity of this result is then investigated further by computing the vibration frequencies associated with the different sites and by comparing the results to the experimental spectra. This comparison allows a reinterpretation of the experimental data and tends to confirm the validity of the bridge site found theoretically. The coadsorption of ethylene and hydrogen on the Pd(110) surface is then investigated with various structures and for different coverages of ethylene and hydrogen. The interaction between hydrogen and ethylene is found repulsive at short range and slightly attractive at long range. Hence, at medium or high coverage, the adsorption of hydrogen decreases the adsorption energy of the ethylene molecule on the surface. Furthermore, the bridge site is more destabilized than the top site with the hydrogen coverage increase: for a monolayer coverage of hydrogen, the two sites have roughly the same energy. An electronic interpretation of this phenomena is given. Finally, the comparison of the computed vibrational frequencies with the experimental results shows that, at low H coverage, the main site is still the bridge one, but that, at a higher coverage, the top site for ethylene becomes competitive.

I. Introduction

The catalytic hydrogenation of ethylene on Pd surfaces is one of the most important processes of industrial chemistry. It has been extensively studied both theoretically^{1–3} and experimentally.^{4,5} The reaction is generally thought to proceed via the Horiuti-Polanyi mechanism,⁶ starting with a strongly rehybridized ethylene molecule. However, the adsorption state of ethylene is an important parameter of the reaction, and recently it was shown from spectroscopic studies⁷ and theoretical calculations⁸ that weakly bound species with a π sp^2 bond character could play an important role on Pt and Pd as precursor states for the hydrogenation reaction. The adsorption state of ethylene on various transition metal surfaces has been the subject of numerous experimental studies,^{9–11} mainly from a spectroscopic approach. We will restrict the discussion here to the case of an adsorption on a Pd(110) surface. Two adsorption sites are generally considered: a top adsorption (also called π) on a metal atom, and a bridge adsorption between two metal atoms, usually associated with a hybridization of the molecule and hence also called di- σ . Vibrational studies do not give direct information on the chemisorption sites, the determination being based on the comparison with frequencies obtained on analogous systems. Such an approach is not straightforward and can lead sometimes to incorrect assignments, as recently shown for the case of NO chemisorption.¹² In the case of ethylene on Pd(110), the most recent studies find, at low coverage, an energy of 178 meV for the C–C stretching mode. The known references are gas-phase ethylene (201 meV) and ethylene in Zeise's salt $K[PtCl_2H_4]Cl_3 \cdot H_2O$ (189 meV). Measurements for ethylene

chemisorbed on metal surfaces give 190 meV for Cu(100), 188 meV for Pd(111), 154 meV for Pt(111), and 150 meV for Ni(111). Hence the shift of the C–C frequency is moderate on Pd(110), compared to the unperturbed molecule, and this leads the authors to conclude that ethylene is π -bonded on Pd(110) (as it was previously done for Cu(100) and Pd(111)), in contrast to the cases of Pt(111) and Ni(111), where a strongly bound di- σ molecule on a bridge site is assumed. Such a conclusion is not completely unambiguous, because the C–C frequency for a given adsorption geometry (e.g., bridge) could be strongly dependent on the nature of the metal surface.

The coadsorption of ethylene with hydrogen is certainly more relevant to the heterogeneous catalysis hydrogenation problem. The presence of hydrogen generally weakens the bonds between ethylene and the surface. For example, on Pt(110), the strongly bound di- σ ethylene species is transformed to a π -bonded species upon coadsorption with hydrogen. On Pd(110), the C–C stretching frequency is shifted from 178 to 186 meV, well in line with a weakening of the molecule–surface interaction. In the case of deuterated ethylene C_2D_4 , two different C–C stretching frequencies appear at 170 and 150 meV, which were associated with the coexistence of two different structures for the molecule on the hydrogenated surface.

Besides vibrational spectroscopy, the adsorption of ethylene on Pd(110) has been studied by LEED and NEXAFS. An ordered $c(2 \times 2)$ pattern was observed. The molecular axis was found to be preferentially aligned along the $[1\bar{1}0]$ row in the case of the adsorption on the bare surface but rotated about the surface normal in the case of the H-covered Pd(110) surface.

Few periodic quantum calculations have studied the adsorption of ethylene on Pd(110), and to our knowledge, none deals

* Corresponding author. E-mail: Daniel.Simon@ens-lyon.fr.

with the coadsorption of ethylene and hydrogen. The work by Pichierri et al.¹³ has concluded that a discrepancy exists between the computed results that show a more stable bridge site and the experimental ones that seem in favor of a π -bonded species on a top site. This contradiction is attributed to wrong trends of the GGA-DFT calculations, which prevent a reliable prediction of the adsorption sites. A study of correlation between adsorption energy and surface structure¹⁴ shows that the bridge site is the most favorable and that the strong relaxation of the Pd (110) surface leads to a significant shift in the level of the metal d-band.

To give some insight to these questions, we present a first principles density functional study of ethylene adsorbed on Pd(110), first without coadsorbed hydrogen, then on a H-covered surface. Our aim is to determine the most stable adsorption structure for ethylene for different possible coverages. The computation of the total energy is supplemented by an electronic interpretation of the adsorption process, and by vibrational calculations. The computed vibration modes are compared to the experimental results and we propose a new assignment of the frequencies.

II. Calculation Method and Computational Conditions

The calculations were performed using the plane-wave density functional theory (DFT) code Vasp^{15,16} with Vanderbilt ultrasoft pseudo-potentials.^{17,18} The exchange-correlation energy and potential are described by the generalized gradient approximation (Perdew–Wang 91¹⁹). Pd surfaces are represented by periodic slabs. A Monkhorst-Pack mesh of $5 \times 3 \times 1$ k -points was used for the (2×2) cell and the k -points density was maintained as constant as possible for the various cell sizes. These slabs are repeated in a supercell geometry with at least 12 Å of vacuum between them. The Pd substrate is made of 6 layers: the 3 lower layers are maintained at DFT-bulk geometry (the Pd–Pd (DFT) distance is 2.81 Å vs 2.75 Å experimentally) and the 3 upper Pd atom layers are allowed to relax. Three different unit cells have been used: (4×2) , (2×2) , and $c(2 \times 2)$ with one ethylene molecule inside and different numbers of H atoms. This allows us to use surface coverages respectively of 0.125, 0.25, and 0.5 monolayer (ML).

The optimization is achieved by using analytical calculations of Hellmann–Feynman forces acting on the atoms of the unit cell. The vibrational calculations were obtained by discrete calculation of the Hessian matrix followed by a diagonalization procedure to obtain the eigenmodes.²⁰

III. Adsorption of Ethylene on Pd(110)

Figure 1 presents the various modes of the adsorption of ethylene on a bare Pd(110) on different adsorption sites. The calculated adsorption energies for the various geometries and coverages are reported in Table 1. The missing values correspond to unstable situations in the case of the top60 case and were not computed for the long bridge case because of the low adsorption energy of this structure.

The bridge structure with the molecular axis aligned along the $[1\bar{1}0]$ is the most stable one, but the top adsorption is only about 0.15 eV higher. For each adsorption geometry top90, top, and bridge, the adsorption energy decreases as the coverage increases. This behavior is fully consistent with steric and surface mediated repulsion between the adsorbed molecules. The average intermolecular minimum H–H distance decreases strongly with the coverage and can have a drastic influence on the stability of the system. At high coverage (0.5 ML), for the most stable bridge chemisorption, a $c(2 \times 2)$ packing is found to be more stable than a (2×1) arrangement by 23 meV/

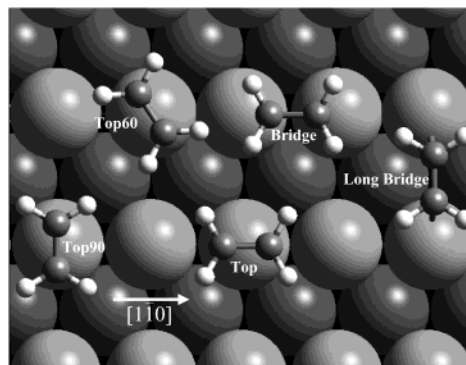


Figure 1. Different adsorption sites of an ethylene molecule on a Pd(110) surface: bridge, top, top60, top90, and long bridge. The lighter Pd atoms belong to the upper surface. The arrow gives the $[1\bar{1}0]$ direction of the surface. The bridge and top adsorbed ethylene are along the $[1\bar{1}0]$ direction, whereas the top60 and top90 adsorbed molecules are tilted by an angle of 60 and 90°, respectively. The long bridge adsorbed ethylene connects two adjacent rows of the Pd (110) surface.

TABLE 1: Adsorption Energy (eV) for Different Ethylene Sites on a Bare Pd(110) Surface as a Function of the Ethylene Coverage^a

coverage	0.125 ML	0.25 ML	0.5 ML
top90	−1.05	−1.01	−0.84
top60			−0.83
top	−1.07	−1.04	−0.96
bridge	−1.21	−1.20	−1.13
long bridge		−0.93	

^a The energy references are the bare Pd(110) surface and the ethylene molecule in the gas phase. The value after “top” indicates the azimuthal angle of the molecule with respect to the $[110]$ direction.

molecule. This can be related to the fact that the H–H intermolecular distances are of 2.13 and 2.17 Å for the bridge (2×1) and $c(2 \times 2)$ arrangements, respectively. In the low concentration (0.125 and 0.25 ML) cases, the top and top90 sites tend to be energetically very close, only separated by 30 meV. However, for the higher coverage (0.5 ML), the top90 site is less stable than the top site by 120 meV. This can be again understood as a strong H–H intermolecular repulsion in this $c(2 \times 2)$ geometry, where two hydrogen atoms have a short intermolecular contact: 1.77 Å for the top90 site, compared to the top (2.14 Å) and the bridge (2.17 Å) sites. Moreover, a top60 orientation is not stable in the low coverage cases but corresponds to a metastable structure at 0.5 ML, because the H–H intermolecular interactions are moderate in this case, with the smallest H–H distance found at 2.57 Å. The long bridge site, calculated only at 0.25 ML, is clearly less stable than other sites (0.93 eV as compared to 1.20 eV for the short bridge site).

Clearly, intermolecular repulsion can also be related to the electronic effects, because, as the coverage increases, the number of surface available electrons that can interact with the π^* system of the ethylene decreases. However, in a first approximation, this effect should be the same for the different sites, in contrast with the steric effect. The electronic effects are discussed in more details below. For the two most stable structures, the C–C bond is oriented along the $[1\bar{1}0]$ rows. The main feature in Table 1 is the fact that the bridge site is always more stable on the Pd(110) surface than the top site, by 144, 168, and 176 meV for the 0.125, 0.25, and 0.5 ML coverages, respectively. This behavior is consistent with previous similar first-principles calculations.¹³ However, the conclusions based on HREELS and STM studies^{21–23} lead to a π -bonded ethylene on a top site. Obviously, a single energy criterion is not

TABLE 2: Geometry of Adsorbed Ethylene on a Bare Pd(110) Surface for Different Sites and Coverages^a

	C–C (Å)	C–Pd (Å)	H tilt angle (deg)	hybridization	Pd–Pd distance (Å) closest to adsorbate
top90 (0.5 ML)	1.39	2.19	16.2	2.24	2.81
top90 (0.25 ML)	1.39	2.21	15.0	2.27	2.81
top90 (0.125 ML)	1.39	2.19	14.1	2.27	2.81
top (0.5 ML)	1.40	2.19	18.1	2.29	2.81
top (0.25 ML)	1.40	2.21	18.0	2.29	2.81
top (0.125 ML)	1.39	2.21	17.8	2.28	2.81
bridge (0.5 ML)	1.44	2.12	33.5	2.50	2.72
bridge (0.25 ML)	1.44	2.13	31.9	2.49	2.73
bridge (0.125 ML)	1.43	2.13	31.8	2.47	2.73
long bridge (0.25 ML)	1.44	2.13	37.6	2.56	3.60

^a The hybridization indicates the relative out-of-plane H tilt angle, planar being assigned a value of 2 (sp^2) and a fragment of ethane, a value of 3 (sp^3). The Pd–Pd distance closest to the adsorbate is the one under the C=C bond for bridge sites and the closest in a row for top sites.

sufficient to supply a convincing theoretical argument, and we will discuss below the vibrational frequency spectrum related to the two kinds of sites.

Before that, we need to point out the geometrical and the electronic features of the adsorbed systems. Table 2 gives the main geometrical aspects of the different sites: the C–C and Pd–C bond lengths, the tilt angle between the CH_2 planes, and the mean plane of the ethylene molecule. This angle is related to a mean hybridization index of the C atomic orbital (sp^2 for 0° , as in the ethylene molecule in the gas phase, sp^3 for 54.7° , as in the ethane gaseous molecule, and a linear interpolation of the hybridization index with the angle between these two limits). The Pd–Pd distances given in Table 2 concern the Pd atoms that are the closest to the ethylene adsorbed molecule. The bridge and top sites obviously correspond to different distortions of the molecule, with a C–C bond length around 1.44 Å for the bridge sites and around 1.39 Å for top sites. This value can be compared to that of the gaseous ethylene molecule, 1.34 Å. The CH_2 plane angle gives a C hybridization of $sp^{2.5}$ for the bridge sites and of $sp^{2.25}$ for the top sites. The C–Pd bond length is slightly shorter for the bridge site (around 2.13 Å) than for the top sites (around 2.20 Å). Therefore, if the adsorption geometry is consistent with a π -bonded ethylene molecule for the top site, the bridge adsorption geometry shows an intermediate distortion of the molecule and does not correspond completely to the large hybridization of an usual di- σ state. In the case of a top adsorption, the nearby Pd–Pd bonds are not significantly affected, whereas for the bridge site the distance between the two Pd atoms of the bridge is shortened by about 0.1 Å. Hence, these two atoms are submitted to a strong adsorption induced strain, to optimize the interaction with the molecule. Moreover, the geometrical deformation of both the molecule and the Pd surface hints for a stronger interaction of ethylene with the bridge site of the Pd(110) surface than with the top sites, because the deviations are larger in the bridge case.

Let us examine the electronic properties of the ethylene adsorbed on the bridge and top sites of Pd (110). The main interactions are dominated, as usual, by the presence of the π (HOMO) and π^* (LUMO) system composed by the in-phase and out-of-phase combinations of the carbon p_z atomic orbitals, respectively, because they are the frontier orbitals, and develop a good overlap with surface orbitals.

The change in the electronic density spatial distribution, as an ethylene molecule is adsorbed in a bridge geometry is presented in Figure 2. Figure 2a shows the decrease of the electronic density: around the ethylene molecule, the loss of electron concerns clearly the π orbital, and the two Pd in direct interaction with the ethylene lose electrons in d_{z^2} -like orbitals. In Figure 2b, an increase of the electronic density is observed on the ethylene, with a π^* -like distribution, and in d_{xz} and d_{yz}

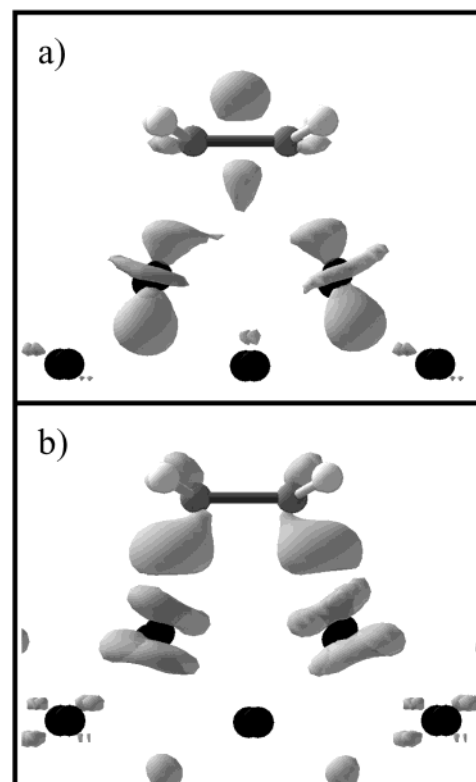


Figure 2. Side view of the differential electron density between a surface with bridge adsorbed ethylene and the superposition of a bare Pd(110) surface and an isolated ethylene molecule, both in the same geometry as in the bridge adsorption site. (a) shows a negative isodensity surface corresponding to the zone of space where the charge is depleted as the ethylene molecule is adsorbed. (b) shows a positive isodensity surface corresponding to the zone of space where the charge increases as the ethylene molecule is adsorbed.

combinations on the Pd atoms. Actually, the zone of increased electronic density on the molecules corresponds to a strongly distorted π^* -like orbital and looks like a combination of two sp^3 orbitals on the carbon atoms. This shape is clearly related to the partial σ character of the bond between the ethylene and the bridge site, in relation with the significant hybridization ($sp^{2.5}$). This contrasts with the π -bond underlined in the case of a bridge ethylene position on the Pt(111) surface.²⁴ Finally, the local character of the electron transfer can be emphasized because only the surface Pd atoms in contact with the carbon atoms show an important density variation.

From the projection of the density of states on combinations of spherical harmonics centered on a given atom, it is possible to represent the local density of states (LDOS) and, therefore, to describe in more detail the nature of the interactions. Figure

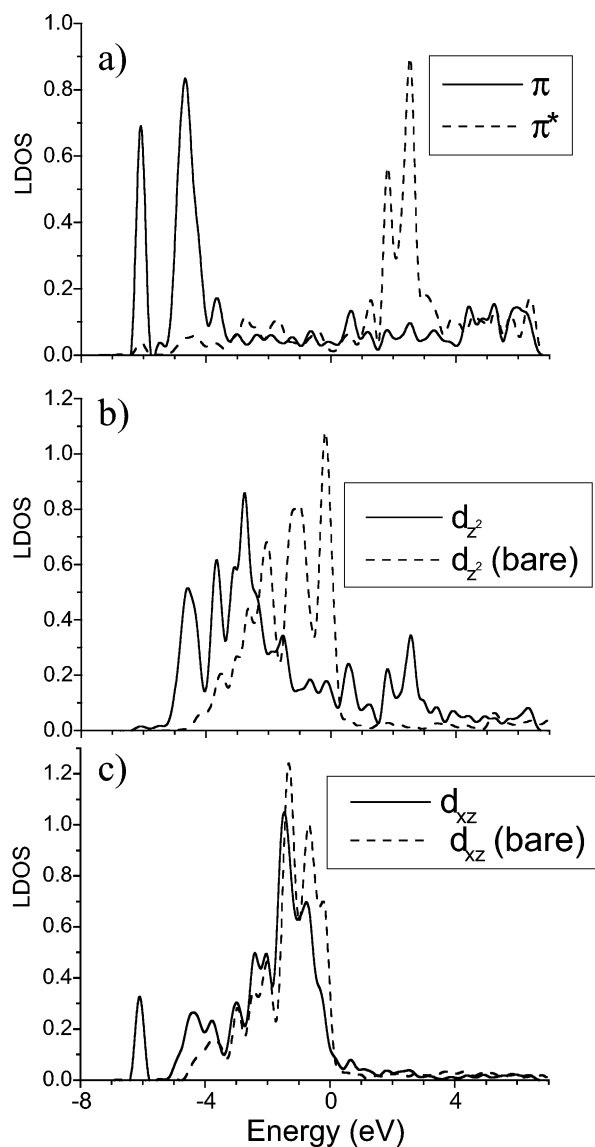


Figure 3. Local densities of states in the case of a bridge ethylene molecule. The zero energy corresponds to the Fermi level. (a) Projection on the ethylene π orbital, defined as the in-phase combination of the p_z orbitals of each C atom (solid line) and on the ethylene π^* orbital defined as the out-of-phase combination of the p_z orbitals of each C atom (dashed line). (b) Projection on the d_{z^2} orbital of a Pd atom in contact with the ethylene molecule (solid line), the reference d_{z^2} projected density of states for a bare Pd(110) surface being a dashed line. (c) Projection on the d_{xz} orbital of a Pd atom in contact with the ethylene molecule (solid line), the reference d_{xz} projected density of states for a bare Pd(110) surface being a dashed line.

3 shows the LDOS curves projected on π and π^* of the ethylene molecule (Figure 3a), on d_{z^2} (Figure 3b) and on d_{xz} (Figure 3c) of the Pd atoms of the site.

The projection on the π and π^* orbitals shows that these states remain close to the eigenvectors for the gaseous ethylene molecule, because they have still intense peaks in the bonding (-4 to -6 eV) and in the antibonding (1 – 3 eV) regions, respectively.

The interaction of π and π^* orbitals is maximum with the d_{z^2} orbitals of the Pd atoms. The π orbital interacts with an in-phase combination of the d_{z^2} orbitals of the bridge site Pd atoms. The LDOS of d_{z^2} has peaks at the same energy as π , the main shared peak being at -4.5 eV. Similarly, the π^* orbital interacts with an out-of-phase combination of the d_{z^2} orbitals of the bridge site Pd atoms. The LDOS of d_{z^2} has peaks at the same energy

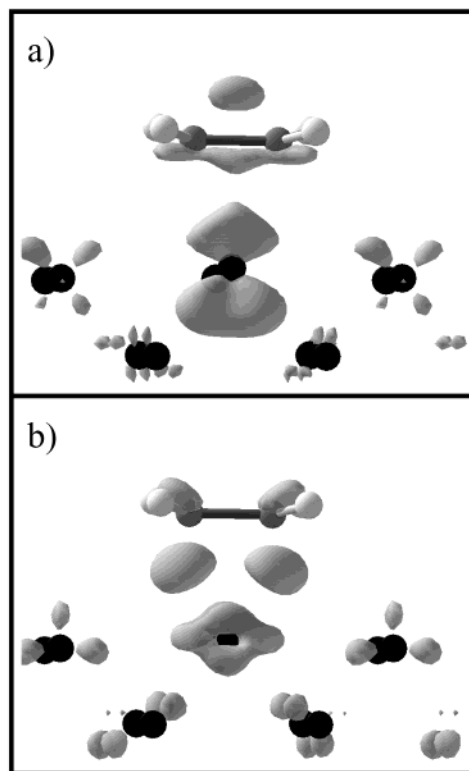


Figure 4. Side view of the differential electron density between a surface with top adsorbed ethylene and the superposition of a bare Pd(110) surface and an isolated ethylene molecule, both in the same geometry as in the top adsorption site. (a) shows a negative isodensity surface corresponding to the zone of space where the charge is depleted as the ethylene molecule is adsorbed. (b) shows a positive isodensity surface corresponding to the zone of space where the charge increases as the ethylene molecule is adsorbed.

as π^* , mainly at $+1.8$ and $+2.5$ eV. These interactions lead to important deformations of the shape of the d_{z^2} band in comparison to the bare Pd(110) surface LDOS. This band is broadened and split into two regions: one at low energy, in the bonding part of the band, and the other just above the Fermi level. As a result, the part close to the Fermi level (between -2 and 0 eV) of the d_{z^2} band is strongly depleted. The low energy part is mainly due to the 2-electron interaction with the π^* orbital. It is stabilizing and results in a fractional electron transfer to π^* . Simultaneously, d_{z^2} states are pushed up above the Fermi level by the 4-electron interaction with π . These states are hence emptied, which increases the strength of the ethylene surface interaction by lowering the antibonding contributions that were just below the Fermi level. Clearly, these two mechanisms result in a depletion of the electronic population of d_{z^2} , which is fully consistent with the negative differential electron density shown in Figure 2a. The ethylene surface bond is therefore a mixing of a π bond involving the d – π interaction, and a di- σ bonding through the d – π^* interaction. It should be underlined here that the π and π^* character is retained to a large extent even for the bridge adsorption geometry, in relation with the partial molecular hybridization. Also, though the molecule is residing on a bridge site, it cannot be referred as a pure di- σ coordination. As seen in Figure 3c, the participation of the d_{xz} orbital is much more moderate, with a main interaction with the π orbital (at -6 eV).

For the case of a top site adsorption, the differential electronic density is shown in Figure 4. The part concerning the ethylene molecule is qualitatively similar to the bridge adsorption case (Figure 2), with a depletion of the π orbital (Figure 4a) and a

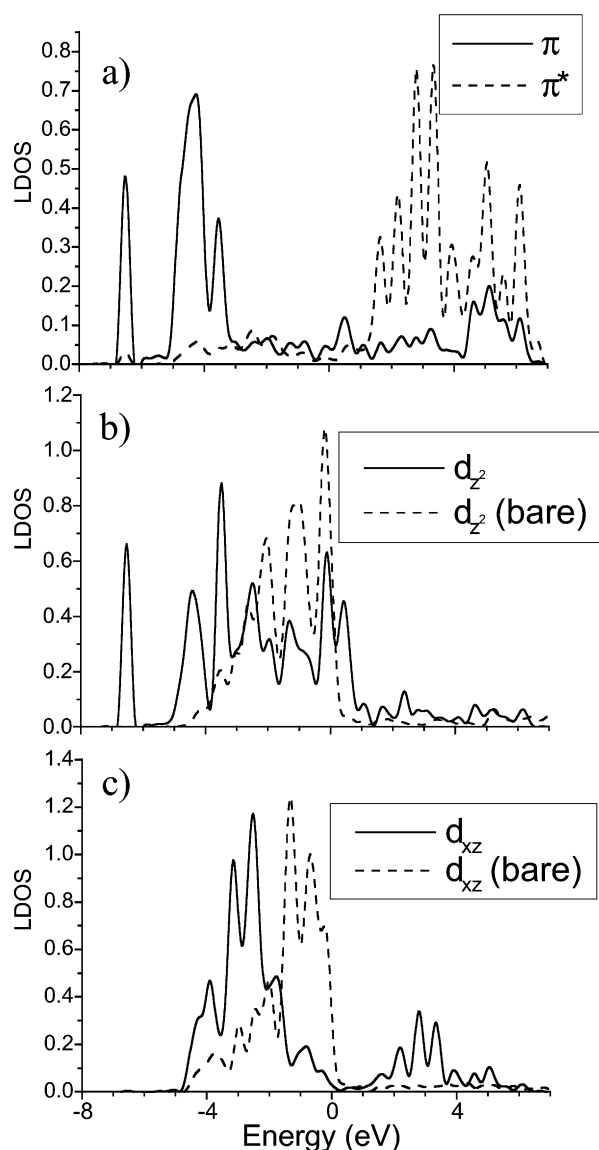


Figure 5. Local densities of states in the case of a top ethylene molecule. The zero energies corresponds to the Fermi level. (a) Projection on the ethylene π orbital, defined as the in-phase combination of the p_z orbitals of each C atom (solid line) and on the ethylene π^* orbital defined as the out-of-phase combination of the p_z orbitals of each C atom (dashed line). (b) Projection on the d_{z^2} orbital of the Pd atom in contact with the ethylene molecule (solid line), the reference d_{z^2} projected density of states for a bare Pd(110) surface being a dashed line; (c) Projection on the d_{xz} orbital of the Pd atom in contact with the ethylene molecule (solid line), the reference d_{xz} projected density of states for a bare Pd(110) surface being a dashed line.

density increase in the π^* one (Figure 4b). The Pd atom directly in contact with the ethylene shows the strongest change in the electronic density: there is a decrease of the density in a combination of d_{z^2} and d_{xz} whereas there is an increase in a combination of d_{yz} and d_{xy} orbitals.

The LDOS of the π and π^* orbitals of the adsorbed ethylene are presented in Figure 5a. The π system shows three main peaks at -6.5 , -4.5 , and -3.5 eV below the Fermi level. These three peaks are also present in the d_{z^2} LDOS, indicating a strong interaction between the d_{z^2} orbital of the metal and the π orbital of the ethylene (Figure 5b). These two orbitals are initially fully (or almost fully) occupied, resulting in the population of antibonding states and a destabilizing interaction. However, some antibonding combinations between the π and d_{z^2} orbitals

are pushed above the Fermi level. This induces a decrease of the electronic density in both the π and d_{z^2} orbitals, as shown in Figure 4a. For the π^* orbital, Figure 5c shows a strong interaction with the d_{xz} band. Bonding states are stabilized; they are mainly centered on the d_{xz} orbital with a small contribution of π^* . As a result, in this case also, the π^* orbital is fractionally occupied. This electronic gain is, however, smaller than in the previous case of the di- σ adsorption. Antibonding states are mainly centered on the π^* orbital with small contributions in the d_{xz} orbital, in relation with the charge decrease on this orbital.

So, in both bridge and top cases, the ethylene–surface bonding can be rationalized by two kinds of interactions. The first one is the 2-electron interaction $d-\pi^*$. There is some electron donation from the Pd d orbitals to the empty π^* orbital of ethylene: this is the usually called back-bonding interaction. The second one is the $d-\pi$ interaction, usually regarded as a 4-electron interaction. In molecular chemistry, this kind of interaction is always repulsive, but in metal surface phenomena, this is not always the case, because a strong $d-\pi$ interaction shifts part of the antibonding states above the Fermi level. Analogous $d-\pi^*$ and $d-\pi$ interactions are involved for the adsorption modes. How can we then understand that the bridge adsorption is yet more stable than the top one? In the case of the bridge site, the overlap between molecular orbitals and the surface seems to be more favorable because the lobes modified by hybridization point in the direction of the metal atoms. This is especially the case for the π^* orbital, and clearly results in a larger electronic transfer, strengthening the interaction between the molecule and the surface. But, more significantly, another reason lies in the capacity of the surface to relax and adapt to the adsorption situation. In the case of the bridge site, the two Pd atoms can reduce their distance from 2.82 to 2.72 Å, to optimize the interaction with the molecule. In the case of the top site the number of degrees of freedom is more limited.

The molecule experiences different geometric deformations upon adsorption on the two different sites, and hence vibrational spectroscopy could be an important tool. The HREELS vibrational spectra of ethylene on Pd(110) have been the subject of several studies,^{9,21,25–27} but the attribution of the frequencies is not straightforward, because the shifts and intensities due to the site geometry and the local symmetry have to be carefully discriminated. We propose a new attribution of the frequencies, based on theoretical calculations, comparatively in the bridge and top geometries. It will allow us to discriminate unambiguously between these two structures.

We use a C_{2v} symmetry for both the bridge and top geometries, with the C–C bond, along the $[1\bar{1}0]$ direction, considered as the y axis. To test the reliability of our results, we have first calculated the vibration frequencies and modes of the ethylene and the deuterated ethylene molecules in the gas phase. Table 3 gives the values, compared to the experimental frequencies.²⁸ The 12 modes are labeled according to the C_{2v} subgroup, whereas the ethylene molecule belongs to the D_{2h} group. To correlate these modes with those of the adsorbed molecule, which is in a C_{2v} symmetry, we will keep the C_{2v} labeling for the vibrational analysis. The agreement between the experimental and the theoretical results is very good, with a difference of 1 or 2 meV except in the case of the C–H and C–D stretching frequencies, where the anharmonicity should be taken into account. Nevertheless, even for these high energy modes the difference is less than 10 and 3 meV in C_2H_4 and C_2D_4 , respectively. Then, we expect, for the adsorbed systems, a proper description of the vibration spectrum, which

TABLE 3: Comparison of the Vibration Energies (meV) in the Ethylene (C_2H_4) and Deuterated Ethylene (C_2D_4) Molecules^a

vibration modes	label, symmetry	C_2H_4 (bridge)	C_2H_4 (top)	C_2H_4 exp ²¹	C_2D_4 (bridge)	C_2D_4 (top)	C_2D_4 exp ²¹	$C_2H_4(g)$ theor (exp) ²⁸	$C_2D_4(g)$ theor (exp) ²⁸
C–H str	ν_5, A_2	394	401	376	283	296	285	395 (385)	289 (286)
	ν_9, B_2	380	404	369	291	299	278	388 (385)	293 (291)
	ν_1, A_1	382	395	361	277	287	265	380 (375)	281 (279)
	ν_{11}, B_1	370	392	353	268	283	271	379 (371)	273 (273)
C=C str	ν_2, A_1	183	187	178	152	167	152	201 (201)	188 (188)
	ν_{12}, B_1	171	175	172	128	129	128	179 (179)	132 (134)
	ν_3, A_1	140	156	137	113	120	112	167 (166)	121 (122)
	ν_6, A_2	151	151	150	119	123	118	150 (153)	123 (125)
rock.	ν_8, B_1	119	107	112–105	94	88	83–78	129 (127)	96 (97)
wag.	ν_7, A_1	109	112	112	79	80	83	117 (118)	88 (89)
twist.	ν_4, A_2	99	112		85	80		116 (117)	91 (90)
rock.	ν_{10}, B_2	116	108	105	72	80	78	103 (102)	74 (73)
Pd–C	ν_{13}, B_2	64	68	64	50	50	47		
	ν_{14}, B_1	47	44	46	45	40	47		
	ν_{15}, A_1	42	38	39	40	37	38		

^a Two adsorption sites, bridge and top, are compared with experimental results. The two last columns give, as a reliability test, the comparison between theoretical and experimental frequencies of the gas phase molecules.

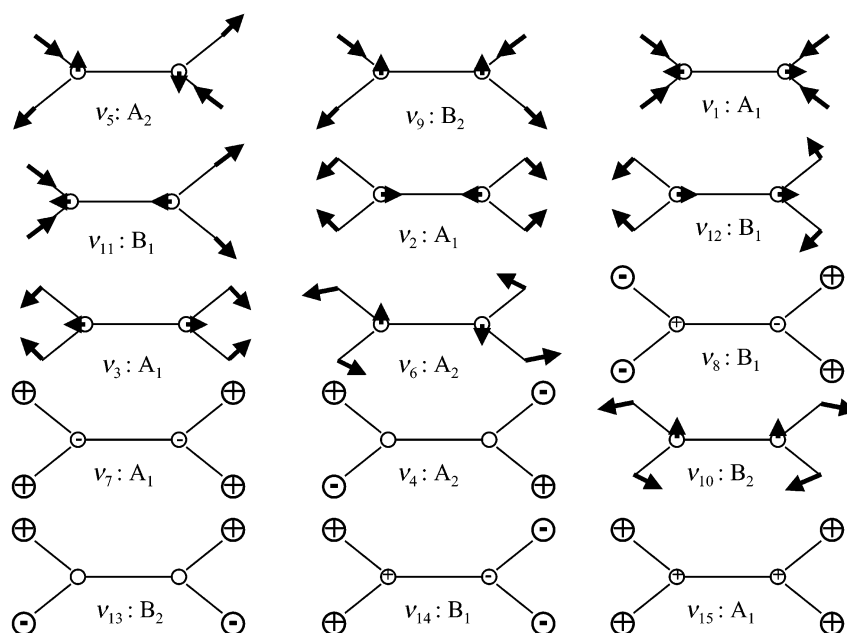


Figure 6. Vibration modes of the ethylene molecule adsorbed on a Pd(110) surface. The arrows correspond to atom displacements in a plane parallel to the surface. The displacement along the z -axis perpendicular to the surface is indicated by + or -. These modes imply mainly the ethylene molecule, the other mode involving Pd atom displacements are found at lower energy. The energies of these modes as a function of the ethylene adsorption site are found in Tables 3 and 7. The symmetry of the vibration modes are given in the C_{2v} space group, and they are sorted according to Tables 3 and 7.

should allow us to propose a pertinent attribution of the experimental frequencies.

The calculated vibration modes are shown in Figure 6. Obviously, the atomic displacements correspond to those of the gaseous ethylene molecules, so we have kept the same ranking of the vibrational modes as in the isolated molecules,²⁸ with a symmetry label in the C_{2v} local adsorption environment. This labeling contrasts with the original numbering,²⁵ which had been given from the Zeise's salt $K[Pt(C_2H_4)Cl_3]H_2O$ vibrational analysis.²⁹ Three modes have been added, due to the metal–ethylene bond, namely a frustrated rotation round the $[1\bar{1}0]$ axis (ν_{13}), a frustrated rotation round the $[001]$ axis (ν_{14}), and a frustrated translation along the axis normal to the surface (ν_{15}). The other low energy modes involving the Pd surface are out of the range of frequencies investigated. Table 3 gives the frequencies values obtained for the bridge and top sites, at a 0.5 ML coverage, in the case of C_2H_4 and C_2D_4 , sorted

according to the frequency value. The comparison with experimental data is given and the proposed attribution will now be discussed, in connection with the HREELS results of Okuyama et al.^{21,27,30} Let us note that the attribution given by Okuyama et al. was based mainly on the comparison with ethylene in Zeise's salt,²⁹ $K[Pt(C_2H_4)Cl_3]H_2O$, and it is revised here in view of the calculated vibrational frequencies.

For the C–H stretching frequencies, the resonant HREELS results allow a clear attribution of frequencies. The anharmonic effects are obvious in the comparison between experimental and theoretical results, with a discrepancy of the same range as in the case of the gas-phase C_2H_4 and C_2D_4 molecules. The other modes need a discussion according to their symmetry.

The A_1 vibrations are excited in the specular mode by a dipole mechanism. They correspond to the main peaks observed in the experimental spectrum, namely, 178 (152), 137 (112), 112 (83), and 39 (38) meV for C_2H_4 (C_2D_4). In the off-specular

modes, these frequencies are also observed but without any notable enhancement or quenching. We attribute them respectively to the ν_2 , ν_3 , ν_7 , and ν_{15} modes of Table 3.

The B_2 vibrations are excited by an impact mechanism in a off-specular mode where the scattering plane is aligned along the [001] direction. In the experimental spectrum, these modes appear at 105 (78) and 64 (45) meV for C_2H_4 (C_2D_4). We attribute these frequencies to the ν_{10} and ν_{13} modes of Table 3. The other peaks in the spectrum are certainly due to a slight distortion in symmetry, but their intensities keep the same proportion, so, we consider that they are not typical off-specular modes.

The B_1 vibrations are excited, by an impact mechanism, in a off-specular mode where the scattering plane is aligned along the [110] direction. In the experimental result, one is obvious at 172 (128) meV, the others are less visible, presumably in the 112–105 (83–78) meV broad peak and doubtless at 46 (45) meV, for C_2H_4 (C_2D_4). We attribute them to the ν_{12} , ν_8 , and ν_{14} modes. Other peaks are visible, but as in the B_2 case, they are likely to be due to an imperfect C_{2v} symmetry.

The A_2 vibrations should not be excited by HREELS in an ideal C_{2v} geometry. The 150 (118) meV low intensity peak for C_2H_4 (C_2D_4) is a good candidate for the ν_6 mode. ν_4 is not observed or hidden by other peaks.

Our attribution differs from the previous one²¹ on the scissoring A_1 , rocking A_2 , wagging B_1 , and the rocking B_2 modes, but it ensures a good correlation with the theoretical frequencies range of the bridge and top adsorption geometries. Furthermore, it is consistent with the relative energies of the two geometries, the bridge one being more stable than the top one. This energetic behavior being true for both molecules, because the C_2D_4 molecule is expected to have the same adsorption site as C_2H_4 (the zero point energy difference in this case is negligible in comparison to the energy difference between bridge and top sites). Indeed, the bridge and top vibrational frequencies differ mainly, in the C_2H_4 case, on the ν_3 mode and, in the C_2D_4 case, on the ν_2 mode, with a difference of more than 15 meV between the theoretical values. In our attribution scheme, the experimental frequencies are fully consistent with the bridge geometry, with 137 meV (as compared to the theoretical value of 140 meV) and 152 meV (identical to the theoretical value) for ν_3 (C_2H_4) and ν_2 (C_2D_4), respectively. Other comparisons may be suggested, but the difference is less marked between bridge and top, leading to a less definite inference.

The overall agreement between theoretical and experimental frequencies is much better in the case of the bridge geometry than in the case of the top geometry. This clearly shows that in the case of ethylene on Pd(110), the measured frequencies are completely compatible with a bridge site structure, mainly because the molecular distortions for this mode remain moderate ($sp^{2.5}$ hybridization), and do not correspond to the complete di- σ bonding scheme. This contrasts with the case of Pt surfaces where the hybridization is much more pronounced in a clear di- σ mode.

Therefore, our frequency analysis is fully consistent with our adsorption energy results that were hinting for a energetically favored bridge site. This contrasts with early interpretations of the spectra that were favoring the top site. Nevertheless, this study of the adsorption of ethylene on pure Pd(110) needs to be completed by the study of the effect of hydrogen coadsorption on this surface, which is a more realistic system: Pd surfaces tend to be polluted very easily, with hydrogen coming from the vacuum residuals or directly from the Pd bulk that is well-

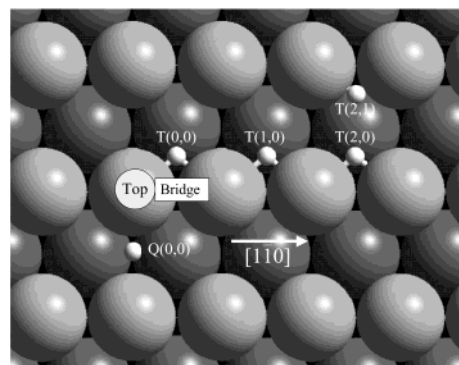


Figure 7. Coadsorption sites of an ethylene molecule and a H atom. Various configurations are presented: a bridge (represented by a box) or a top (represented by a circle) site for the ethylene molecule and 3-fold sites, labeled T(i,j) or 4-fold sites, labeled Q(i,j) for the H atom. The various positions of the H atom are indicated by the value of (i,j) where i is the rank of the H site along the [110] direction, in the row j relative to the ethylene molecule site.

known for its affinity with hydrogen. Moreover, the coadsorption of ethylene with atomic hydrogen is a precursor system toward the catalytic hydrogenation of unsaturated hydrocarbons.

IV. Coadsorption of Ethylene and Hydrogen

To focus on the properties of a realistic system precursor to the hydrogenation reaction, the coadsorption of ethylene and hydrogen has been investigated. Hydrogen adsorption on a Pd(110) surface has been previously studied^{31,32} and the most stable site was found to be the pseudo-3-fold one in the grooves. We have built, on the basis of the main ethylene adsorption states, i.e., top and bridge, a coadsorbed phase in which the hydrogen atoms are either in 3-fold sites, in 2-fold sites on the rows, or in 4-fold sites in the grooves. Figure 7 gives the different hydrogen sites that have been studied here: the various ternary sites are labeled as a function of their position with respect to the ethylene molecule, referred as top or bridge. Although relaxation was fully allowed, no reconstruction of the surface has been investigated in this work. The Pd(110) coadsorbed surface could be metastable, as is the hydrogen-covered surface.³² Nevertheless, the mutual influence of ethylene and hydrogen, which is the aim of the study, may be assumed as little influenced by the reconstruction. In this work the effect of the coadsorption is considered through three questions: what is the influence on the adsorption energy of the distance between the ethylene molecule and the hydrogen atom? What is the geometry of the hydrogen phase? How are the adsorption site and the ethylene geometry affected by the hydrogen coadsorption?

A. Low Coverage. The low coverage case allows us to understand the effect of the coadsorption on the ethylene adsorption energy as a function of the distance between the ethylene molecule and the hydrogen atom. We have used a (4×2) unit cell, with one ethylene molecule and one hydrogen atom coadsorbed, which corresponds to a coverage of 0.125 ML for each. For an ethylene molecule in the bridge site, the H position has been changed by probing various 3-fold sites (noted here T). Table 4 gives the ethylene adsorption energy and geometry of various coadsorption configurations, using the hydrogenated surface as an energy reference. On the bare surface, the H atom adopts a 3-fold site in the side of the trough. In the case of the bridge site, the adsorption energy of ethylene was studied as a function of the separation with the hydrogen atom. In the (4×2) cell, the most stable situation corresponds to the largest separation in the same row. The adsorption energy

TABLE 4: Ethylene Adsorption Energy (eV) on a H-Covered Pd(110) Surface (0.125 ML Coverage) for Various Geometry Arrangements^a

	E_{abs} (eV)	C–C (Å)	C–Pd (Å)	Pd–Pd(C ₂ H ₄) (Å)	Pd–Pd (H) (Å)	H–Pd ₍₂₎ (Å)
top T(0,0)	−0.93	1.39	2.22		2.88	1.74
top90 T(0,0)	−0.95	1.39	2.23		2.90	1.77
bridge T(0,0)	−0.88	1.43	2.15	2.75	2.75	1.69
bridge T(1,0)	−1.21	1.43	2.14	2.71	2.89	1.81
bridge T(2,0)	−1.26	1.43	2.13	2.73	2.91	1.84
bridge T(2,1)	−1.24	1.44	2.13	2.73	2.91	1.83

^a The energy reference is that of the H-covered surface with the ethylene molecule in the gas phase. Typical distances (in Å) are given: C–C bond length, C–Pd distance between a carbon atom and the nearest Pd, Pd–Pd(C₂H₄) distance between the two Pd atoms of the bridge site, Pd–Pd(H) distance of two Pd atoms in the 3-fold H site, H–Pd₍₂₎ distance between the hydrogen atom and the nearest Pd atom of the second layer.

TABLE 5: Ethylene Adsorption Energy (eV) on a H-Covered Pd(110) Surface (0.25 ML Coverage) for Various Geometrical Arrangements^a

	E_{ads} (eV)	C–C (Å)	C–Pd (Å)	Pd–Pd (C ₂ H ₄) (Å)	Pd–Pd (H) (Å)	H–Pd ₍₂₎ (Å)
top T(0,0)	−0.83	1.39	2.22		2.86	1.75
top90 T(0,0)	−0.89	1.39	2.22		2.87	1.75
bridge T(0,0)	−0.83	1.43	2.15	2.76	2.76	1.69
bridge T(1,0)	−1.11	1.42	2.15	2.70	2.91	1.78
top Q(0,0)	−0.92	1.38	2.21			1.85
top90 Q(0,0)	−0.91	1.39	2.21			1.85
bridge Q(0,0)	−1.07	1.43	2.14	2.73		1.87

^a The energy reference is that of the H-covered surface with the ethylene molecule in the gas phase. Typical distances (in Å) are given: C–C bond length, C–Pd distance between a carbon atom and the nearest Pd, Pd–Pd(C₂H₄) distance between the two Pd atoms of the bridge site, Pd–Pd(H) distance of two Pd atoms in the 3-fold H site, H–Pd₍₂₎ distance between the hydrogen atom and the nearest Pd atom of the second layer.

is however slightly improved compared to the case of the bare surface, or when the ethylene and the hydrogen are in different rows, indicating a small attractive interaction for such long distances. A correct description of this subtle effect would require a larger cell; nevertheless this long-range attraction effect can be the consequence of the interaction between the opposite strain fields induced by the hydrogen and ethylene in the Pd surface. A strong destabilization occurs if the hydrogen is moved closer to the ethylene (+0.4 eV for bridge T(0,0)), with a small elongation of the C–Pd bond. This destabilization with a short proximity to the hydrogen atom is also seen for the top site, but the decrease of adsorption energy compared to the bare surface is smaller (0.24 eV). The top T(0,0) then becomes 50 meV more stable than the bridge: the relative stabilities are inverted, suggesting a possible effect of H on the ethylene adsorption site, at higher coverage.

B. Intermediate Coverage. A higher coverage of both ethylene and hydrogen was considered by using a (2 × 2) unit cell (0.25 ML of both ethylene and hydrogen). The various geometry configurations may allow us to understand the behavior of the ethylene molecule and its adsorption site in the presence on a H-covered surface. The results are given in Table 5. The strongest adsorption is on a bridge site with a hydrogen in the T(1,0) pseudo-hollow site, but a bridge site with a hydrogen atom displaced in a 4-fold Q(0,0) position is very close in energy (40 meV). All the other adsorption sites are at least 150 meV less stable.

The adsorption energy of ethylene decreases when the hydrogen coverage is increased. The bridge T(1,0) is, for example, destabilized by 100 meV between coverages of 0.125 and 0.25 ML. The top90 structure, the most stable top adsorption site, is only destabilized by 60 meV. Hence the bridge site is more sensitive to an increase of hydrogen coverage. The adsorption geometry and distances are not strongly modified compared to the low coverage case. Nevertheless, in the case of the bridge-T(1,0) configuration, the strength of the Pd–H bond seems to be reinforced because the Pd–H distance decreases from 1.81 Å (Table 4) to 1.78 Å (Table 5). This destabilization of the ethylene molecule can be seen as a

competition with the H atom, toward the interaction with the Pd surface. This results in a repulsion between the ethylene molecule and the H atom, through the Pd surface. In view of this behavior, an important point remains: the increase of the hydrogen coverage changes the energy difference between the ethylene bridge and top sites; could the bridge ethylene site become unstable at an even higher coverage of hydrogen?

C. High Coverage. Our model is a (2 × 2) cell, with one ethylene molecule (0.25 ML) and 4 hydrogen atoms, which corresponds to a 1 ML H-coverage. At this H-coverage and at low temperature, the stable reconstruction of hydrogen on Pd(110) surfaces is a zigzag pattern (Zg),³¹ with the H atoms in 3-fold sites, on alternating sides of the rows. Another configuration can be envisaged where the H atoms are located in a line on the same side of the row (Ln). Ethylene was positioned in the top and bridge sites, starting with these two kinds of H configuration: Zg and Ln (Figure 8). The results for the adsorption energies and for the main geometry features are presented in Table 6.

The coadsorption with ethylene does not change the preference for H to adopt a Zg pattern and the Ln arrangement of H atoms is still less stable, by about 200 meV. All ethylene adsorption energies are further reduced compared to the intermediate coverage case. The most stable site is still the bridge site, but the most stable top site is only 30 meV higher in energy. The ethylene molecule is not oriented perpendicular to the Pd row anymore, but it is rotated by 52° with respect to this [110] direction. The energy difference is strongly reduced in comparison to the case of the adsorption of ethylene on a bare Pd(110) surface, where the bridge is more stable than the top sites by 170 meV.

The calculation precision, the zero point energy and the entropic effect should be carefully considered with such a small energy difference. The calculation validity was investigated by increasing the numerical precision (fft, charge grids, number of *k*-points, plane wave cutoff) and by testing a new pseudo-potential (PAW potentials),^{33,34} nevertheless no drastic change for the relative stability of these two sites was observed. It should be stressed, however, that 30 meV is certainly smaller than the

TABLE 6: Ethylene Adsorption Energy (eV) on a H-Covered Pd(110) Surface (1 ML Coverage) for Various Geometry Arrangements^a

	E_{ads} (eV)	C–C (Å)	C–Pd (Å)	Pd–Pd (C ₂ H ₄) (Å)	Pd–Pd (H) (Å)	H–Pd ₍₂₎ (Å)
top (Zg)	−0.72	1.38	2.25		2.82	1.741
top52 (Zg)	−0.79	1.38	2.25		2.82	1.77
bridge (Zg)	−0.82	1.42	2.19	2.72	2.90	1.73
top (Ln)	−0.53	1.39	2.23			1.85
top90 (Ln)	−0.53	1.39	2.22			1.84
bridge (Ln)	−0.57	1.42	2.16	2.72		1.85

^a Zg and Ln correspond respectively to zigzag and line H configuration (see Figure 8). The energy reference is that of the Zg H-covered surface with the ethylene molecule in the gas phase. Typical distances (in Å) are given: C–C bond length, C–Pd distance between a carbon atom and the nearest Pd, Pd–Pd(C₂H₄) distance between the two Pd atoms of the bridge site, Pd–Pd(H) distance of two Pd atoms in the 3-fold H site, H–Pd₍₂₎ distance between the hydrogen atom and the nearest Pd atom of the second layer.

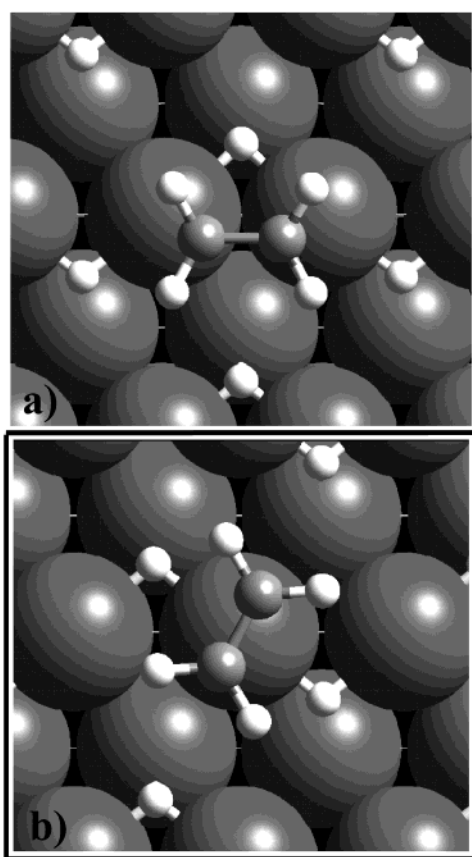


Figure 8. Coadsorption sites of one ethylene molecule and four H atoms in a (2 × 2) cell. The coverage is 0.25 and 1 ML for ethylene and hydrogen, respectively. (a) bridge(Zg) configuration, where the ethylene molecule is in a bridge site and the H atoms adopt a zigzag (Zg) pattern. (b) top52(Zg) configuration, where the ethylene molecule is in a top52 site and the H atoms adopt a zigzag (Zg) pattern.

systematic error in the adsorption energy, associated with the approximate exchange-correlation functional in DFT. Hence, from the energy calculation itself, it is not possible to conclude unambiguously on the relative stability of the bridge and top adsorption sites.

The structure of these two coadsorption sites is presented in Figure 8, and the details of the characteristic distances are given in Table 6. The local symmetry of the bridge-Zg is C_s : the ethylene molecule is tilted by 12.2° from the mean surface plane, hinting for a strong repulsion between ethylene and the closest hydrogen. The azimuthal angle of 52° in the top52 site allows us to minimize the repulsion between the ethylene molecule and the hydrogen atoms. The local symmetry is close to C_{2v} . These two changes in the geometry of the molecule should be a consequence of the modification in the electronic structure of

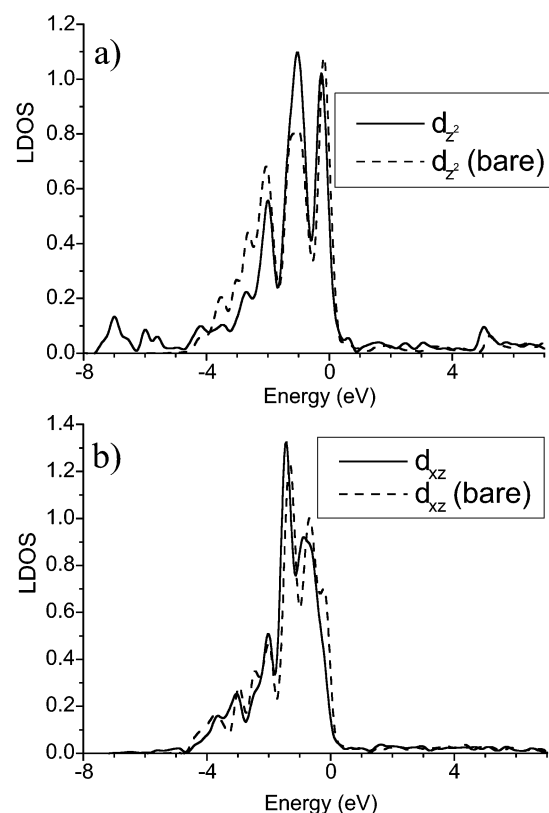


Figure 9. Local densities of states in the case of a 1 ML (Zg) configuration of the H atoms, adsorbed on a Pd(110) surface. The zero energy corresponds to the Fermi level. Projection on (a) a d_z^2 orbital and (b) a d_{xz} orbital of a surface Pd atom (solid line). The dashed lines are the same projections for a bare Pd(110) surface.

the surface due to the adsorption of hydrogen. These changes are related to the weakening of the adsorption of ethylene on this hydrogenated surface.

D. Electronic Interpretation. To give an explanation of the changes in ethylene adsorption features due to the presence of surface-hydrogen, we will compare the electronic densities of states associated to the orbitals involved in the chemisorption process.

A first step toward the understanding of the change of the adsorption properties on hydrogenated surfaces, is to illustrate the modification induced by the hydrogen on the electronic structure of Pd surface atoms. The H-covered surface is in a Zg configuration, as previously, and the density of states is projected on the Pd atoms of the first layer. In Figure 9 we focus on the projected density of states on the d_z^2 and d_{xz} orbitals that will be the main ones involved in the chemisorption of ethylene. They are compared to the case of a bare Pd(110) surface, taken as a reference. In Figure 9a, the LDOS of the d_z^2

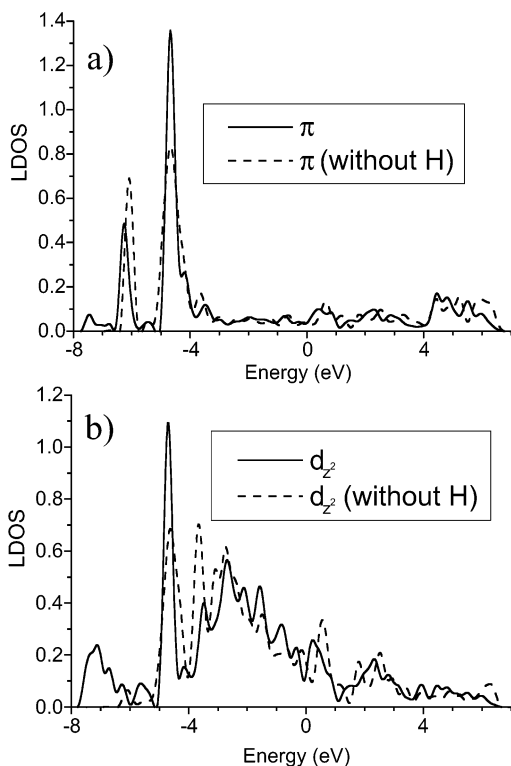


Figure 10. Local densities of states in the case of a bridge(Zg) configuration (Figure 8a). The zero energy corresponds to the Fermi level. (a) Projection on the π orbital of the ethylene molecule (solid line), the same orbital for the surface without hydrogen (Figure 3a) is presented in dashed line. (b) Projection on a d_{z^2} orbital of the surface Pd atom in contact with the ethylene molecule (solid line), the same orbital for the surface without hydrogen (Figure 3b) is presented in dashed line.

orbital is strongly modified by the presence of hydrogen, with new peaks appearing around -7 , -6 , and $+5$ eV from the Fermi level. Those peaks correspond to interaction and mixing with the s orbital of the H atoms. A decrease of the width of the Pd d-band can also be observed. This is associated with a shift of the d-band center to higher energies by about 40 meV. In Figure 9b, the LDOS of the d_{xz} orbital is much less affected by the presence of hydrogen: we notice a slight decrease of the d-bandwidth, but with an unchanged d-band center, which lowers the contributions close to the Fermi energy.

Let us consider first the bridge-Zg configuration. This case is illustrated in Figure 10, where the π LDOS of ethylene in the presence of hydrogen is compared to the LDOS without surface hydrogen atoms (Figure 10a). Three features are noticeable. The first one is the broad peak around -7 eV. It is obviously due to the presence of hydrogen and corresponds to the interaction between H and the π orbital of ethylene, mediated by the Pd atoms. The second point is the decrease of the contribution at -6 eV. It corresponds to a lowering of the interaction with d_{xz} orbitals, because as seen in the first part of this paper (Figure 3), this peak is shared mainly by the π and d_{xz} orbitals. The third feature concerns the peak common to the π and d_{z^2} orbitals (Figure 10a,b, respectively), at -4.6 eV: this peak is raised. The interpretation of this behavior is based on the 4-electron interaction between H and the low energy contributions of π . This interaction tends to split the energy levels into two contributions, at lower and higher energy (associated respectively to the peaks at -7 and -4.6 eV). This interaction is repulsive, because it takes place at energies very far from the Fermi level: the peak associated with antibonding

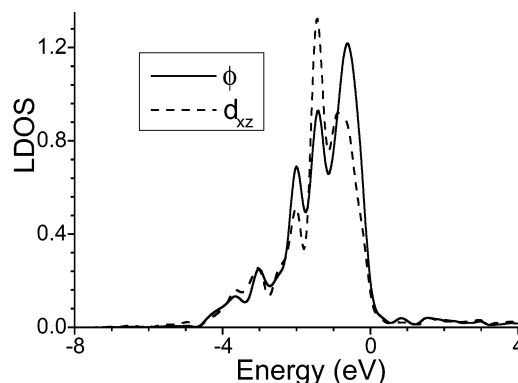


Figure 11. Local density of states projected on the orbital ϕ , combination of d_{xz} and d_{yz} Pd orbitals interacting with the π^* orbital of the ethylene molecule, in a top52(Zg) coadsorption configuration (Figure 8b) (solid line). The reference d_{xz} is presented in dashed line.

mixing remains below the Fermi level and hence is occupied. This is a kind of steric repulsion that pushes the ethylene molecule away from the hydrogen atom that shares the same bridge adsorption site (Figure 8a). Actually, this repulsion is not direct, through space, but takes place through the metal surface atoms.

Furthermore, the donation interaction from the Pd d_{z^2} and d_{xz} bands to the π^* orbital of the ethylene is weakened, because the d_{z^2} band center is shifted to lower energy from the interaction with the H (Figure 9). This interaction is a classical 2-electron stabilizing interaction whose weakening induces a decrease of the adsorption of the ethylene on the hydrogenated surface. Then, the strong adsorption energy decrease of the ethylene on the hydrogenated Pd surface is the consequence of both the increase of the repulsive 4-electron $d_{z^2}-\pi$ interaction and the decrease of the bonding $d_{z^2}-\pi^*$ interaction.

Let us now look at the top52-Zg configuration (Figure 8b). The same kind of steric 4-electron repulsion may be put forward, for the top geometry. The d_{z^2} orbital is the one most affected by the interaction with H atoms: there is a strong increase of the LDOS for the lower energy, particularly around the one of the π orbital of the ethylene. This is consistent with a strong 4-electron repulsion $\pi-d_{z^2}$ as in the case of the bridge site. This strong repulsion should be the leading cause of the decrease of the adsorption energy for all the top sites (by 250 meV) on the hydrogenated surface in comparison to a bare Pd surface.

However, in contrast to the bridge site case, the strongly modified d_{z^2} orbital does not interact with the π^* orbital for the top adsorption. In the top ethylene, the π^*-d_{xz} bonding is only weakly decreased by the adsorbed H from a downshift of the d_{xz} peak close to the Fermi level. This effect is minimized by the rotation of the ethylene to the more stable geometry top52. In this site, the π^* orbital of the ethylene interacts with an orbital ϕ , combination of d_{xz} and d_{yz} , which has a negligible overlap with the H atoms orbitals: these H atoms are more or less in the nodal plane of ϕ . This orbital ϕ (Figure 11) shows a higher contribution to the LDOS close to the Fermi level than the d_{xz} , inducing a stronger interaction: hence, the rotation of the ethylene by 52° allows a stronger donation from the metal surface to the π^* of the ethylene and stabilizes the adsorption.

In conclusion, both top and bridge sites show a strong decrease of the adsorption energy mostly induced by the increase of the 4-electron repulsion between the π orbital of the ethylene and the d_{z^2} band of the metal caused by the adsorbed H. However, whereas, for the bridge site, the donation interaction between d_{z^2} and π^* is weakened by the presence of the H, in the case of the top52 site, the donation interaction is preserved

TABLE 7: Comparison of the Vibration Energies (meV) for Ethylene (C_2H_4) and Deuterated Ethylene (C_2D_4) Molecules, Chemisorbed on the Pd (110) Surface, in the Presence of 1 ML Coadsorbed Hydrogen^a

vibration mode	label, symmetry	$C_2H_4, 4H$ (bridge)	$C_2H_4, 4H$ (top52)	$C_2H_4(g)$ exp_1^{21}	$C_2H_4, 4H$ (bridge)	$C_2H_4, 4H$ (top52)	$C_2H_4(g)$ exp_1^{21}	$C_2H_4(g)$ exp_2^{27}
C—H str	ν_5, A_2	384	388		286	289		
	ν_9, B_2	387	392	377	288	291	(284)	
	ν_{11}, A_1	373	380	365	272	278	272	275/268
	ν_{11}, B_1	372	378		269	273		
C=C str	ν_2, A_1	180	187	186	155	169	166	170/153
	ν_{12}, B_1	172	175	174	127	130	(—)	
	scis	143	155	151	114	117	118	118
	ν_3, A_1	143	155		114	117		
	rock.	147	146		117	118		
	wag.	113	113		91	90		
	ν_8, B_1	113	113		91	90		
	wag.	104	112	113	77	84	84	82
	twist.	104	116		75	81		
	ν_4, A_2	104	116		75	81		
Pd—C	ν_{10}, B_2	107	99		74	71		
	ν_{13}, B_2	62	64	69	46	46	(50)	
	ν_{14}, B_1	51	42	44	45	37		—/48
	ν_{15}, A_1	39	36	38	38	35	37	35

^a Two coadsorption sites, bridge-Zg and top52-Zg, are compared with experimental results, exp_1^{21} and exp_2^{27} obtained at 1 ML hydrogen, 0.1 ML ethylene coverage for exp_1 , and 1 ML hydrogen, saturation in ethylene, for exp_2 .

by the rotation of the molecule allowing the interaction with a combination of d_{xz} and d_{yz} , which is mostly unchanged by the presence of H. The top52 site is then less destabilized by the adsorbed H than the bridge site. This explains why top site adsorption becomes competitive on a surface preadsorbed with a high coverage of H.

E. Vibrational Calculations. The vibrational spectra of ethylene and deuterated ethylene adsorbed on a hydrogenated surface has been studied experimentally^{21,27} and a comparison with theoretical results should help us to compare the two bridge-Zg and top52-Zg configurations, with very similar energies, which have been underlined previously. The results are presented in Table 7, still with the symmetry attribution of a C_{2v} group, although the geometry of both bridge and top52 configurations is distorted.

First, if we compare these results to those in the absence of hydrogen (Table 3), we see that the vibrational energies are mainly unchanged. The main differences are observed for C—H and C—D (ν_5 , ν_9 , ν_{11} , and ν_{11}) with an energy decrease of 10–15 meV (except C_2D_4 (bridge) with a change less than 5 meV). The other modes have a variation of a few millielectronvolts, which may not be considered as significant. The ν_{10} mode is an exception, with a decrease of about 9 meV. There is no direct relationship with the decrease of adsorption energy of the ethylene molecule. This could be related to the fact that the 4-electron interaction, mainly responsible for the molecule destabilization, is not associated with any net charge transfer either from or toward the ethylene orbitals. Hence, it has no strong influence on the bond strength within the molecule. As in the previous analysis, made for C_2H_4 and C_2D_4 in the absence of hydrogen, our results may lead to a discrimination between the bridge-Zg and the top52-Zg configurations. Indeed, the ν_2 , ν_3 , and, to some extent, ν_7 frequencies clearly differ between the two configurations, either in C_2H_4 or in C_2D_4 or in both cases. Then, we can attribute, from these calculations, the experimental peaks of two different cases labeled exp_1 and exp_2 , respectively, in Table 7: the first experiment corresponds to an ethylene coverage of 0.1 ML and a saturation coverage for H,²¹ the second one corresponds to a saturation coverage for both ethylene and hydrogen.²⁷ In the case of C_2H_4 , the experimental ν_2 value, 186 meV, corresponds to top52-Zg, 187 meV (180 meV for bridge-Zg). Moreover, in the C_2D_4 case, exp_1 gives 166 meV, corresponding to top52 at 169 meV, whereas bridge gives 155 meV. The second experiment, exp_2 ,

provides two peaks, at 170 and 153 meV, in good agreement with the coexistence of two phases, that we can attribute respectively to the top52-Zg and bridge-Zg configurations. The ν_3 C_2H_4 frequency confirms the main attribution of the exp_1 peak, 151 meV, to the top52-Zg, computed at 155 meV. The C_2D_4 frequencies are too close to allow a clear-cut conclusion for ν_3 . In the ν_7 vibration mode, the conclusion is still the same: the top52-Zg configuration (respectively 112 and 84 meV in C_2H_4 and C_2D_4) has a good correlation with the experimental values (respectively 113 and 84 meV). So, the conclusion is clear: the attribution based on exp_1 hints for a top52-Zg coadsorption structure, whereas exp_2 allows, at high ethylene coverage, a possible mixing of both bridge-Zg and top52-Zg coadsorption sites. This behavior is fully consistent with our adsorption energy results, which show that the high concentration of hydrogen on the surface destabilizes the bridge site more than the top site, leading to an equivalent adsorption energy.

V. Conclusion

The calculated energies and frequencies, and the comparison with experimental data, clearly show that the adsorption site of ethylene on a Pd(110) surface is modified by hydrogen coadsorption. On a bare Pd(110) surface, the lowest energy site for ethylene is the bridge site, 170 meV more stable than the other possible ones. Furthermore, experimental vibrational energies agree with the calculated vibrations for this bridge site, in contrast with former experimental attributions of spectra that lead to a top site. Hence, both energy and frequencies indicate that for ethylene the bridge site is preferred on a bare (or weakly hydrogenated) Pd(110) surface. In this bridge site, the hybridization of the molecule toward sp^3 remains intermediate and hence this bridge structure cannot be referred to as a complete di- σ case. The situation is different on the hydrogenated Pd(110) surface (1 ML, (2×1) -H). The bridge and the top adsorption modes have very similar total energies, with a difference of only 30 meV. The calculated frequencies, compared to experimental data, show that the molecule resides on a top site at low coverage (0.1 ML) of ethylene, whereas high coverages of ethylene can be associated to a mixture of top and bridge sites.

The clear trend is that hydrogen coadsorption weakens the interaction between the ethylene molecule and the surface. Hydrogen and ethylene compete for the interaction with the surface metal atoms, and Pd states stabilized by combination with H 1s orbitals show a reduced ability to couple with ethylene

states. The associated repulsion is smaller for the top site, hence leveling the energies, because the molecule has the freedom to rotate to maximize its overlap with Pd d states that are only weakly affected by H preadsorption. In such cases where the adsorption energies are similar, it is not possible to conclude from the energy alone, due to a limited accuracy. The calculation of molecular properties, such as vibrational frequencies, and their comparison with experimental data is then a powerful tool. This modified adsorption mode of ethylene on a hydrogen covered Pd surface has potential consequences on the reactivity of the molecule toward hydrogenation by favoring some reactions pathways. The understanding of the pathways of the hydrogenation on the Pd(110) surface is the next step that is under investigation and should allow us to understand the exceptional reactivity of a more complex structure like deposit surfaces of Pd on Ni(110).^{35–37}

Acknowledgment. This work was supported by the *Région Rhône-Alpes* under Contract No. 70006614 and by the computational resource center IDRIS (CNRS) under contracts No. 001064 and 0609.

References and Notes

- (1) Neurock, M.; van Santen, R. *J. Phys. Chem.* **2000**, *104*, 11127.
- (2) Neurock, M.; Venkataraman, P. D.; van Santen, R. A. *J. Am. Chem. Soc.* **2000**, *122*, 1150.
- (3) Hansen, E. W.; Neurock, M. *J. Catal.* **2000**, *196*, 241.
- (4) Bos, A.; Bootsma, E.; Foeth, F.; Sleyster, H.; Westerterp, K. *Chem. Eng. Process* **1993**, *32*, 53.
- (5) Sekitani, T.; Takaoka, T.; Fujisawa, T.; Nishijima, M. *J. Phys. Chem.* **1992**, *96*, 8462.
- (6) Huriuti, J. *Trans. Faraday Soc.* **1938**, *30*, 1164.
- (7) Cremer, P.; Su, X.; Shen, Y.; Somorjai, G. *Catal. Lett.* **1996**, *40*, 143.
- (8) Pallassana, V.; Neurock, M. *J. Catal.* **2000**, *191*, 301.
- (9) Nishijima, M.; Yoshinobu, J.; Sekitani, T.; Onchi, M. *J. Chem. Phys.* **1989**, *90*, 5114.
- (10) Cassuto, A.; Mane, M.; Jupille, J. *Surf. Sci.* **1991**, *249*, 8.
- (11) Delacruz, C.; Sheppard, N. *J. Chem. Soc., Chem. Commun.* **1987**, 1854.
- (12) Loffreda, D.; Simon, D.; Sautet, P. *Chem. Phys. Lett.* **1998**, *291*, 15.
- (13) Pichierri, F.; Iitaka, T.; Ebisuzaki, T.; Kawai, M.; Bird, M. *J. Phys. Chem.* **2001**, *105*, 8154.
- (14) Ge, Q.; Neurock, M. *Chem. Phys. Lett.* **2002**, *358*, 377.
- (15) Kresse, G.; Hafner, J. *Phys. Rev. B* **1994**, *49*, 14251.
- (16) Kresse, G.; Furthmüller, J. *Comput. Mater. Sci.* **1996**, *6*, 15.
- (17) Vanderbilt, D. *Phys. Rev. B* **1990**, *41*, 7892.
- (18) Kresse, G.; Hafner, J. *J. Phys.: Condens. Matter* **1994**, *6*, 8245.
- (19) Perdew, J. P.; Chevary, J. A.; Vosko, S. H.; Jackson, K. A.; Pederson, M. R. *Phys. Rev. B* **1992**, *46*, 6671.
- (20) Filhol, J.-S. Ph.D. Thesis, Ecole Normale Supérieure de Lyon, France, 2001.
- (21) Okuyama, S.; Ichihara, S.; Ogasawara, H.; Kato, H.; Komeda, T.; Kawai, M.; Yoshinobu, J. *J. Chem. Phys.* **2000**, *112*, 5948.
- (22) Ichihara, S.; Ogasawara, H.; Nantoh, M.; Komeda, T.; Kawai, M.; Domen, K. *Electron Spectrosc. Relat. Phenom.* **1998**, *88*, 1003.
- (23) Ogasawara, H.; Ichihara, S.; Okuyama, H.; Domen, K.; Kawai, M. *Electron Spectrosc. Relat. Phenom.* **2001**, *114*, 339.
- (24) Ge, Q.; King, D. A. *J. Chem. Phys.* **1999**, *110*, 4699.
- (25) Chesters, M. A.; McDougall, G. S.; Pemble, M. E.; Sheppard, N. *Appl. Surf. Sci.* **1985**, *22*, 369.
- (26) Nishijima, M.; Sekitani, T.; Yoshinobu, J.; Onchi, M. *Surf. Sci.* **1991**, *242*, 493.
- (27) Ichihara, S.; Ogasawara, H.; Kato, H.; Komeda, T.; Kawai, M.; Domen, K. *Chem. Lett.* **2000**, *2*, 112.
- (28) Shimanouchi, T. *Tables of Molecular Vibrational Frequencies*; NSRDS-NBS: Washington, DC, 1972.
- (29) Hiraishi, J. *Spectrochim. Acta A* **1969**, *25*, 749.
- (30) Okuyama, H.; Ichihara, S.; Kato, H.; Yoshinobu, J.; Kawai, M. *Chem. Phys. Lett.* **1999**, *310*, 451.
- (31) Ledentu, V.; Dong, W.; Sautet, P.; Kresse, G.; Hafner, J. *Phys. Rev. B* **1998**, *57*, 12482.
- (32) Dong, W.; Ledentu, V.; Sautet, P.; Eichler, A.; Hafner, J. *Surf. Sci.* **1998**, *411*, 123.
- (33) Bloch, P. E. *Phys. Rev. B* **1994**, *50*, 17953.
- (34) Kresse, G.; Joubert, J. *Phys. Rev. B* **1999**, *59*, 1758.
- (35) Filhol, J.-S.; Simon, D.; Sautet, P. *Phys. Rev. B* **2001**, *64*, 85412.
- (36) Filhol, J.-S.; Saint-Lager, M.-C.; Santis, M. D.; Dolle, P.; Simon, D.; Baudoing-Savois, R.; Bertolini, J.; Sautet, P. *Phys. Rev. Lett.* **2002**, *89*, 146106.
- (37) Porte, L.; Phaner-Goutorbe, M.; Guigner, J.; Bertolini, J.-C. *Surf. Sci.* **1999**, *424*, 262.